Progress In Electromagnetics Research, PIER 58, 243–269, 2006

FORWARD PROPAGATION MODELING ABOVE GAUSSIAN ROUGH SURFACES BY THE PARABOLIC WAVE EQUATION: INTRODUCTION OF THE SHADOWING EFFECT

V. Fabbro

ONERA-DEMR
2 Avenue Edouard Belin, 31055 Toulouse Cedex 4, France

C. Bourlier

IREENA, Ecole Polytechnique de l'Université de Nantes
Rue Christian Pauc, La Chantrerie
BP 50609, 44306 Nantes Cedex 3, France

P. F. Combes

UPS-AD2M-IGEEP
118 Route de Narbonne, 31062 Toulouse Cedex 4, France

Abstract—In this paper, a fast method is presented to model the forward propagation above Gaussian rough surfaces and taking into account atmospheric refraction. The method is based on the Discrete Mixed Fourier Transform (DMFT) solved by the Parabolic Wave Equation, in which the Ament boundary condition with shadowing effect is used at grazing angle. In this model, for a bistatic configuration, the surface height PDF of the illuminated points is derived and it is introduced in the boundary condition. Examples demonstrate the capacities of the method to compute propagation factor above rough surfaces following Gaussian statistics and Gaussian height correlation and the proposed method is validated by comparison to a Monte Carlo approach.

1. INTRODUCTION

To model electromagnetic wave propagation in the troposphere and above rough surfaces, it is necessary to take into account various interaction phenomena of the wave with the propagation medium. Indeed, absorption, diffusion, refraction or diffraction are able to disturb the wave propagation above earth's surface. To predict radar detection and telecommunications connection range in operational conditions, hybrid modeling techniques of the propagation have been developed, e.g., AREPS [1], TERPEM [2]. These hybrid methods use PWE resolution technique to model propagation at low altitudes. Since many years, the Parabolic Wave Equation (PWE) has been used to model the electromagnetic or acoustic wave propagation in inhomogeneous medium. In all cases (above ocean or mountain for example) the boundary conditions play an essential role and must be modeled accurately. This point is the main advantage of the PWE, because the method is "full wave" and takes into account intrinsically the boundary conditions, modeling all the interaction phenomena of the wave with the surrounding medium. In addition, it has been observed that propagation modeling above rough sea can lead to an over-estimation of the radar detection range. In order to reduce this over-prediction, the introduction of shadowing effect is proposed here.

The goal of this paper is to propose a fast and efficient method for operational use, predicting the forward propagation above rough surfaces and taking into account the shadowing and refraction effects. To solve rigorously the electromagnetic scattering problem from rough surfaces, computational methods based on method of moments [3–5], could be applied; but these techniques are very time consuming and it is not the purpose of this paper.

The forward scattering process is computed from the asymptotic theory based on the Ament model [6]. This leads to the main advantage of our method that is fast and requires a computation time of the amount of few seconds for any case. Freund et al. [7] showed that the propagation factors obtained from a Monte Carlo process by method of moments and the Ament model are shifted: the minima and maxima positions of the interference figure are different at grazing angles. We will show in this paper, that this phenomenon is due to the fact that the shadowing effect is not taken into account. In this paper, the rough surface reflection coefficient developed by Ament [6] is improved by including the shadowing effect, which is very important especially at low grazing angles.

In Section 2, the resolution of the PWE in two dimensions applying the Split Step Fourier method (SSF) is presented. According to the

impedance boundary conditions, the Discrete Mixed Fourier Transform (DMFT) developed by Dockery and Kuttler [8] is presented within a short description of the irregular terrain modeling. In Section 3, the shadowing effect at grazing angle is presented for Gaussian statistics, and the height Probability Density Function (PDF) of the illuminated points is derived analytically in the forward direction. This study leads to a new height PDF of the illuminated points, in which the mean value and the standard deviation of the illuminated surface heights are calculated. In addition, the analytical approach is compared with a Monte-Carlo method. In Section 4, a new reflection coefficient is derived from the height PDF presented in Section 3. The interest of the proposed approach is proven and discussed in Section 5 by comparison with a statistical Monte Carlo approach on several examples. Finally, Section 6 gives concluding remarks on the performances of the proposed method, its applicability to different type of surfaces and further improvements are also proposed.

2. PARABOLIC WAVE EQUATION RESOLUTION

2.1. Introduction

Numerous methods are available to model electromagnetic wave propagation in the atmosphere, e.g., geometrical optics, and mode theory. However, the complicated variations of the refractive index and the presence of the ground limit the applications of these methods. An alternative solution is to use a numerical method to solve the parabolic approximation of the Helmholtz equation.

The Parabolic Wave Equation (PWE) is the most popular method to compute electromagnetic propagation in the troposphere at low altitudes. The PWE was originally developed by Fock [9] but was not a practical solution until Hardin and Tappert [10] developed a simple solution in acoustics based on the Fourier transform called Split-Step Fourier method. Its robustness and accuracy for complicated problems with vertical and horizontal index variation made it a computational powerful method. The formulation of the PWE for electromagnetic problems is summarized by Kuttler and Dockery [8, 11]. The theory of the PWE has already been explained in detail [11–14] and will not be reported here. Numerous approaches were developed to solve the PWE with some differences in the approximation of the pseudo differential operator. The wide angle PWE proposed by Donohue and Kuttler [13] is used here:

$$\frac{\partial \Phi}{\partial x} = j\sqrt{k_o^2 + \frac{\partial^2}{\partial z^2}}\Phi + jk_o m(x,z)\Phi, \tag{1}$$

where x is the horizontal range, z the altitude, k_o the free-space wave number, $m(x,z)$ the modified refractive index and $\Phi(x,z)$ the scalar tangential electric or magnetic field for horizontal or vertical polarization, respectively. Here, we assume $\exp(-j\omega t)$ time dependency of the fields.

Several methods can be used to solve the PWE. The more efficient in term of computation time is based on the Fourier transform: it is the Split-Step Fourier method (SSF). The principle is a recursive resolution with range, following the formulation given below:

$$\Phi(x+\delta x,z) = e^{j\frac{k_o}{2}m(x,z)\delta x}\mathcal{F}^{-1}\left\{e^{j\delta x\sqrt{k_o^2-p^2}}\mathcal{F}\left[e^{j\frac{k_o}{2}m(x,z)\delta x}\Phi(x,z)\right]\right\}. \tag{2}$$

$\mathcal{F}$ is the Fourier operator, p the dual of z in the spectral domain and δx the horizontal step length.

2.2. Boundary Condition

To model the propagation above high-conducting surfaces, according to the wave polarization, the boundary conditions of Dirichlet (horizontal polarization) or Neumann (vertical polarization) have to be enforced. However, for many problems, considering the ground as perfectly-conducting is not a good approximation. The solution usually applied in PWE approach is to introduce the Leontovitch boundary condition [15].

The Leontovitch boundary condition [15] states that

$$\left.\frac{\partial\Phi}{\partial z}\right|_{z=0} + \alpha_{H,V}\Phi|_{z=0} = 0, \tag{3}$$

$\alpha_{H,V}$ can be directly obtained from the Fresnel reflection coefficient R and the grazing angle ϕ (defined from the horizontal direction) such as:

$$\alpha_{H,V} = jk_o\sin(\phi)\frac{1-R(\phi)}{1+R(\phi)}. \tag{4}$$

We will show in Section 4 that this expression allows to introduce the roughness and the shadowing effect of the surface along the propagation direction.

Expression (4) has a strong dependence with the local grazing angle ϕ, which generally depends on the refractive index and on the local geometry of the scene. Many approaches can be used to estimate this angle, e.g., Geometrical Optics (GO) and Spectral Approximation (SA) [14]. To obtain the most accurate grazing angle, it is necessary

to use a combination of both approaches according to the specific condition under which they are valid.

The SSF method is based on a Fourier transform of the field along the z-axis (cf. Equation (2)). It could be noticed that a sine Fourier transform of the field gives an exact solution of the Dirichlet boundary condition (enforcing the field equal to zero on the ground) and by analogy a cosine transform satisfies the boundary condition of Neumann. The objective of the Discrete Mixed Fourier Transform (DMFT), derived by Kuttler and Dockery [8], is to find a solution which will apply the boundary condition of Leontovich (4), (5) by combining the conditions of Neumann and Dirichlet. Thus, a matched function ψ is introduced defined as

$$\psi = \frac{\partial \Phi}{\partial z} + \alpha_{H,V}\Phi, \tag{5}$$

where ψ is a function which satisfies both the Parabolic Wave Equation and the boundary condition of Leontovich if $\psi(x, 0) = 0$. Then ψ can be propagated using (2) and with a sine transform. To obtain ψ, the above equation can be rewritten with finite difference expression of the partial derivative. With this method, the impedance boundary condition is automatically propagated and propagation above rough surface can be studied.

2.3. Deterministic Irregular Terrain Modeling

Accurate modeling of radiowave propagation over deterministic irregular terrain (relief) is crucial in this study to validate the results above rough surfaces obtained using the modified impedance by comparison with a Monte Carlo approach. The last one consists in modeling the propagation above series of deterministic surfaces and the average of the propagated fields is computed.

The "Staircase terrain approach" models the ground profile as series of plane surfaces located at different heights. The propagation above each flat surface is calculated by the DMFT dependent on the boundary condition. The origin of the vertical sampling of the field is shifted according to the height variation of the profile. This method considers the field as zero inside the obstacle and above the calculation domain. This technique is not based on any mathematical formulation but on intuitive concept. Barrios [12] demonstrated the accuracy of the staircase approach if the transmitter and the receiver are at low altitude. However, cutting the relief in a series of staircases fails to take into account the reflection of the field on the obstacles, so another more accurate technique is to use a shift map in the iterative resolution approach to model irregular terrain.

The "Shift map approach", applied by Donohue and Kuttler to the PWE technique [13], assumes smooth terrain given by a simple change of variable binding the profile of the ground with the resolution of the Helmholtz equation. The result is a global equation, solved by the DMFT, which directly propagates the field obeying to the Leontovitch boundary condition and above the surface profile. The SSF recursive resolution becomes:

$$\begin{aligned}\Phi(x+\delta x,z) &= e^{j\frac{k_o}{2}\tilde{m}(x,z)\delta x+\phi'} \\ &\mathcal{F}^{-1}\left\{e^{j\delta x\sqrt{k_o^2\cos^2\beta-p^2}}\mathcal{F}\left[e^{j\frac{k_o}{2}\tilde{m}(x,z)\delta x-\phi'}\Phi(x,z)\right]\right\}. \quad (6)\end{aligned}$$

In this process, at each iteration the slope β of the surface is taken into account. In this formulation, a new modified refractive index is introduced :

$$\tilde{m}=\sqrt{m^2-\sin^2\beta}, \quad (7)$$

and a phase correction is applied at each iteration of the process :

$$\phi'=jk_oz\sin\beta. \quad (8)$$

This way, the boundary conditions becomes :

$$\psi=\frac{\partial\Phi}{\partial z}+\gamma_{H,V}\Phi, \quad (9)$$

with

$$\gamma_{H,V}=\cos\beta\left[\alpha_{H,V}+(1-\cos\phi)\tan\beta\right]. \quad (10)$$

Nevertheless, Donohue and Kuttler tested this approach above several wedges and showed that this method is valid only if the slope of the wedge is lower than 15 degrees. They explained that the sources of this breakdown were clearly identified as split-step solution errors, due to the paraxial limitation of the PWE resolution method. This is why both approaches for modeling irregular terrain are coupled in order to obtain a more accurate result, alternating the shift mapping if the surface slope is less than 15 degrees and the staircase approach for higher slope values.

3. SHADOWING MODELING AT GRAZING ANGLE

3.1. Introduction

In this section, the height Probality Density Function (PDF) of the illuminated points is derived considering Gaussian statistics and the case of the forward propagation. The mean value and the standard

deviation of the surface illuminated heights are also derived and numerical results are presented for small grazing incidence angle ϕ. In addition, the model is compared with a Monte-Carlo method and validated.

3.2. Illumination Height PDF

As depicted in Fig. 1 for grazing incidence angles ϕ, due to the shadowing effect, only a portion of the total surface is illuminated. The purpose of this section is to calculate the *illumination* height PDF which is different of the height PDF.

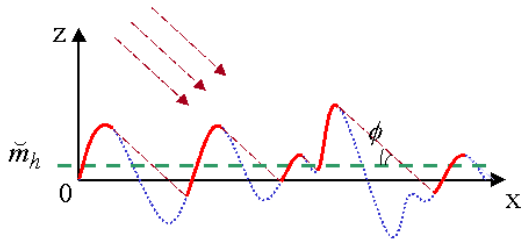

Figure 1. Illustration of the mean height of a rough surface illuminated by a plane wave of incidence ϕ.

The problem of wave scattering from a rough surface in the presence of shadowing was first considered analytically by Bass and Fuks [16, 17] by means of the theory of random function overshoots developed in Ref. [18]. The statistical (this means that the averaging over the surface slopes and heights is not performed) illumination function was then expressed from an infinite Rice series (for more details see Ref. [19]). The shadowing effect was rediscovered later, seemingly independently, with the Wagner [20], Smith [21, 22] and Beckman [23] formulations, who retained the first term of the series. Moreover, Smith used the Wagner approach by introducing a normalization function.

For monostatic and bistatic configurations, these authors assumed a one–dimensional surface with an *uncorrelated* Gaussian process of surface heights and slopes. This means that the statistical illumination function is independent of the surface height correlation function. Recently, for one- and two-dimensional surfaces with Gaussian statistics, Bourlier et al. [19, 24] extended the Wagner and the Smith formulations by taking into account the correlation. For moderate incidence angles, they showed that the correlation could be neglected. Moreover, they showed by comparing the Wagner and

the Smith formulations with a Monte-Carlo method that the Smith approach is more accurate than the Wagner is.

In this subsection, by considering Gaussian statistics and the forward direction, the illumination height PDF is derived by using the Wagner and the Smith approaches with and without correlation. In order to keep the best formulation, these approaches are compared with a Monte-Carlo method for small grazing angles.

When the shadowing effect is taken into account, the illumination height PDF is written as

$$\breve{p}(\phi;\xi) = \frac{\displaystyle\int_{-\infty}^{+\infty} p_\gamma(\gamma) S(\phi;\xi,\gamma) d\gamma}{\displaystyle\int_{-\infty}^{+\infty}\int_{-\infty}^{+\infty} p_{\xi,\gamma}(\xi,\gamma) S(\phi;\xi,\gamma) d\xi d\gamma} p_\xi(\xi), \tag{11}$$

in which p_γ and p_ξ are the slope and the height PDF, and $p_{\xi,\gamma}$ is the joint height PDF of the surface heights and slopes. $S(\phi;\xi,\gamma)$ is the statistical illumination function of an arbitrary point of the surface of height ξ and slope γ observed with a grazing incidence angle ϕ. At the denominator, the double integral corresponds to the normalisation function such as $\int_{-\infty}^{+\infty} \breve{p}(\phi;\xi) d\xi = 1$. If the points of the surface are all illuminated then $S = 1$ and the unshadowed height PDF if found such as $\breve{p}(\phi;\xi) = p_\xi(\xi)$.

3.2.1. Illumination Height PDF for Any Uncorrelated Process

In the forward direction and for *any uncorrelated* random process, the use of the Wagner, S_W, and the Smith, S_S, formulations lead to [19]

$$\begin{cases} S_W(\phi;\xi) = \left(\exp\left\{-\Lambda(\phi,\sigma_s)\left[1 - F(\xi)\right]\right\}\right)^2 \\ S_S(\phi;\xi) = \left\{\left[F(\xi)\right]^{\Lambda(\phi,\sigma_s)}\right\}^2 \end{cases}. \tag{12}$$

For a bistatic configuration, S_W and S_S are defined as the product of two monostatic statistical illumination functions. In the forward direction, since the incidence angles of the transmitter and the receiver are equal in absolute value, the monostatic statistical illumination function with respect to the transmitter and the receiver are equal. This explains the power 2 in the above equation. We can note that S_W and S_S do not depend on the surface slope γ. F stands for the height cumulative function defined as

$$F(\xi') = \int_{-\infty}^{\xi'} p_\xi(\xi) d\xi, \tag{13}$$

where p_ξ is the height PDF. Λ is expressed as

$$\Lambda(\phi, \sigma_s) = \frac{1}{\tan\phi} \int_{+\tan\phi}^{+\infty} (\gamma - \tan\phi) p_\gamma(\gamma) d\gamma, \tag{14}$$

where p_γ is the slope PDF. Substituting (12) into (11) and integrating over the heights ξ and the slopes γ, we show for any uncorrelated process that

$$\begin{cases} \breve{p}_W(\phi;\xi) = p_\xi(\xi) \dfrac{2\Lambda}{1-\exp(-2\Lambda)} \exp\left\{-2\Lambda\left[1-F(\xi)\right]\right\} \\ \breve{p}_S(\phi;\xi) = p_\xi(\xi)(1+2\Lambda)\left[F(\xi)\right]^{2\Lambda} \end{cases}. \tag{15}$$

For Gaussian statistics, we have $p_\xi(\xi) = \frac{1}{\sigma_\xi\sqrt{2\pi}} \exp\left(-\frac{\xi^2}{2\sigma_\xi^2}\right)$ and $p_\gamma(\gamma) = \frac{1}{\sigma_\gamma\sqrt{2\pi}} \exp\left(-\frac{\gamma^2}{2\sigma_\gamma^2}\right)$ with σ_ξ and σ_γ the standard deviations of the surface heights and slopes (the mean values are assumed to be equal to zero), respectively. From (14) and (13), this leads to

$$\begin{cases} \Lambda(\phi, \sigma_s) = \Lambda(v) = \dfrac{\exp(-v^2) - v\sqrt{\pi}\mathrm{erfc}(v)}{2v\sqrt{\pi}} \quad v = \dfrac{\tan\phi}{\sqrt{2}\sigma_\gamma} \\ F(\xi) = 1 - \dfrac{1}{2}\mathrm{erfc}\left(\dfrac{\xi}{\sqrt{2}\sigma_\xi}\right) \end{cases}. \tag{16}$$

In conclusion, the illumination height PDF for any uncorrelated process, $\breve{p}_{W,S}(\phi;\xi) \equiv \breve{p}_{W,S}(v;\xi)$, depends on the surface height ξ and on the parameter v.

3.2.2. Illumination Height PDF for a Correlated Gaussian Process

For a correlated Gaussian process, Bourlier et al. [19] showed that the statistical illumination functions of Wagner, S_W, and Smith, S_S, are expressed as

$$S_{W,S}(\phi;\xi,\gamma) = \left\{ G_{W,S}(\phi;\xi,x_t) \exp\left[-\int_0^{x_t} g_{W,S}(\phi;\xi,\gamma,x) dx \right] \right\}^2. \tag{17}$$

The functions $G_{W,S}$ and $g_{W,S}$ are expressed in Appendix A. x is the horizontal distance between two points on the surface. x_t is the distance above which the correlation between two points on the surface can be neglected. For a Gaussian surface height correlation, $x_t = 3L_c$, where L_c is the surface height correlation length. For the simulations,

it is convenient to use the variable transformations given by (A1). Substituting (17) into (11), one obtains the illumination height PDF with correlation, in which $p_{\xi,\gamma}(\xi,\gamma) = \frac{1}{2\pi\sigma_\xi\sigma_\gamma}\exp\left(-\frac{\xi^2}{2\sigma_\xi^2} - \frac{\gamma^2}{2\sigma_\gamma^2}\right)$. The introduction of the correlation requires the computation of three fold numerical integrations over $\{x, \gamma, \xi\}$.

3.2.3. Illumination Height PDF from a Monte-Carlo Method

To keep the formulation as accurate as possible, the different approaches will be compared with a Monte-Carlo method. The algorithm is based on the work of Brokelman and Hagfors [25]. It is summarized in Table 5. of [19], in which it is extended to a bistatic configuration. The method is briefly summarized. Firstly, for a given surface height correlation function, the surface heights are generated by using a spectral method. Secondly, for a given grazing incidence angle, if a point of the surface of index p is illuminated by the transmitter, then the boolean value of $I_1(p) = 1$, $I_1(p) = 0$ otherwise. Thirdly, the same way is used for the receiver, in which the surface heights is flipped because the ray emanates from the right; one obtains $I_2(p)$. Thus, a point of the surface is illuminated if it is viewed both by the receiver and the transmitter. Thus $I = (I_1 \text{ and } I_2)$. The illuminated heigths correspond to the indexes, p, for which $I(p) = 1$.

3.3. Numerical Results

For the Monte-Carlo method, to obtain a number of points sufficient to predict the illuminated height PDF, the number of samples is equal to one million and the surface height correlation length is $L_c = 200$ units.

In Fig. 2, the illumination normalized height PDF $\breve{p}(h;\phi) = \sqrt{2}\sigma_\xi \breve{p}(\xi;\phi)$ is plotted versus the surface normalized heights, $h = \xi/(\sqrt{2}\sigma_\xi)$, for $\phi = 3$ degrees and $\sigma_\gamma = 0.1$ ($L_c = \sqrt{2}\sigma_\xi/\sigma_\gamma$).

Five approaches are displayed: Monte-Carlo (MC), Smith without correlation (Un smith), Smith with correlation (Co Smith), Wagner without correlation (Un Wagner), Wagner with correlation (Co Wagner). The unshadowed normalized height PDF, $\exp(-h^2)/\sqrt{\pi}$, is also depicted. In the legend, the mean value, $\breve{m}_h$ (dimensionless), and the standard deviation, $\breve{\sigma}_h$ (dimensionless), of the illuminated normalized height are also reported. They are defined from $\breve{p}(h;\phi)$

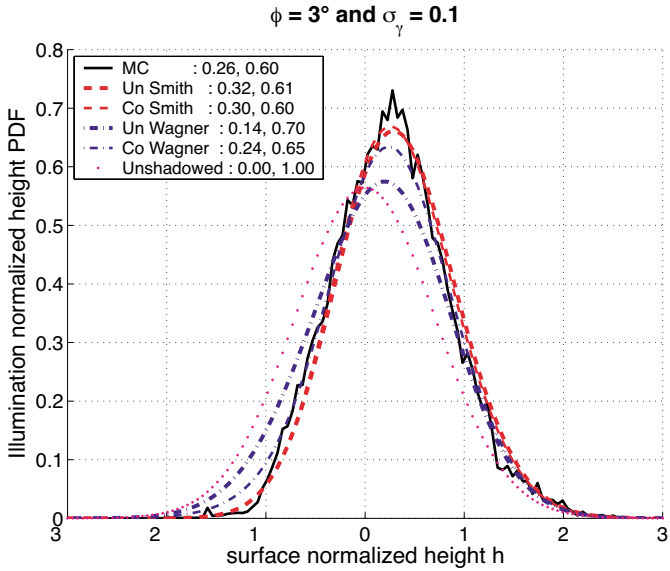

Figure 2. Illumination normalized height PDF $\breve{p}(h;\phi) = \sqrt{2}\sigma_\xi \breve{p}(\xi;\phi)$ versus the surface normalized heights, $h = \xi/(\sqrt{2}\sigma_\xi)$, for $\phi = 3$ degrees and $\sigma_\gamma = 0.1$.

as

$$\begin{cases} \breve{m}_h = \displaystyle\int_{-\infty}^{+\infty} h\breve{p}(h;\phi)dh \\ \breve{\sigma}_h^2 = \displaystyle\int_{-\infty}^{+\infty} (h-\breve{m}_h)^2 \breve{p}(h;\phi)dh \end{cases} . \tag{18}$$

We can note that

$$\breve{m}_\xi = \sqrt{2}\sigma_\xi \breve{m}_h \text{ in m} \qquad \breve{\sigma}_\xi = \sqrt{2}\sigma_\xi \breve{\sigma}_h \text{ in m.} \tag{19}$$

In Fig. 2, we observe that the Smith approach is better than the Wagner approach, for which the mean value $\breve{m}_h$ is slightly underestimated and the standard deviation $\breve{\sigma}_h$ is weakly overestimated. The mean value predicted by the Smith approach is very close to the one obtained with the Monte-Carlo method. In addition, since the deviation between the correlated and the uncorrelated Smith results is small, in the following of the paper, we will keep only the *uncorrelated Smith approach*. Further simulations, not reported in this paper, confirms this choice. Fig. 2 also shows that the shadowing effect

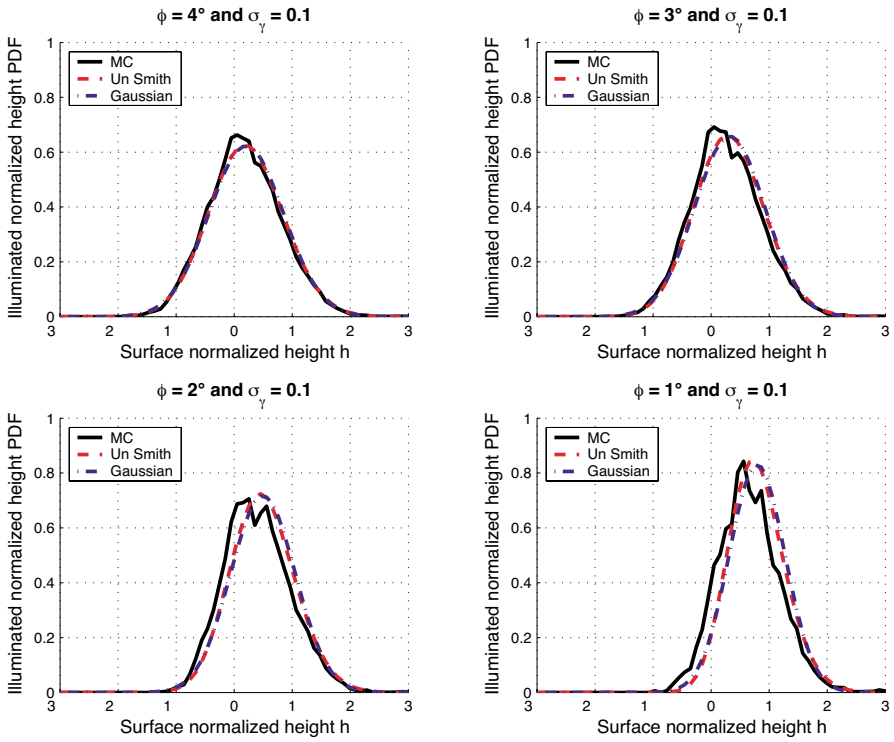

Figure 3. Comparison of the illumination normalized height PDF $\breve{p}(h;\phi)$ witha Gaussian profile versus the surface normalized heights, $h = \xi/(\sqrt{2}\sigma_\xi)$, for $\phi = \{4, 3, 2, 1\}$ degrees and $\sigma_\gamma = 0.1$.

strongly affects $\breve{m}_h > 0$ and $\breve{\sigma}_h$. Indeed, if the shadowing effect is omitted then $\breve{m}_h = 0$ and $\breve{\sigma}_h = 1/\sqrt{2}$ since $\breve{\sigma}_\xi = \sqrt{2}\sigma_\xi\breve{\sigma}_h = \sigma_\xi$ for any grazing incidence angle ϕ.

Fig. 2 reveals that the shape of the illumination normalized height PDF is close to a Gaussian PDF. From this simple observation, $\breve{p}(h;\phi)$ can be fitted as

$$\breve{p}(h;\phi) = \frac{1}{\breve{\sigma}_h\sqrt{2\pi}} \exp\left[-\frac{(h-\breve{m}_h)^2}{2\breve{\sigma}_h^2}\right], \tag{20}$$

In Fig. 3, the illumination normalized height PDF $\breve{p}(h;\phi)$ is compared with the Gaussian profile versus the surface normalized heights, $h = \xi/(\sqrt{2}\sigma_\xi)$, for $\phi = \{4, 3, 2, 1\}$ degrees and $\sigma_\gamma = 0.1$. A very good agreement is observed between the Monte-Carlo and the uncorrelated Smith results and the Gaussian profile. With the uncorrelated Smith

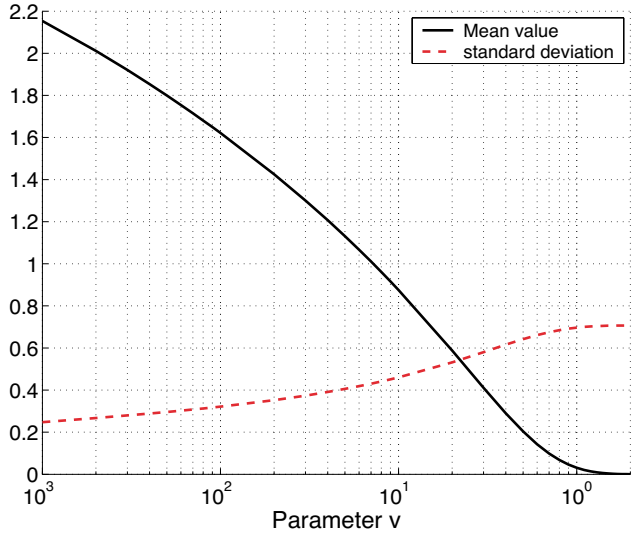

Figure 4. Mean value, $\breve{m}_h$, and standard deviation $\breve{\sigma}_h$ of the illumination normalized heights versus the parameter $v = \tan\phi/(\sqrt{2}\sigma_\gamma)$.

formulation, substituting (15) into (18) and using (16), $\breve{m}_h$ and $\breve{\sigma}_h$ are given by

$$\begin{cases} \breve{m}_h(v) = \dfrac{1+2\Lambda}{\sqrt{\pi}} \displaystyle\int_{-\infty}^{+\infty} h e^{-h^2} \left[1 - \mathrm{erfc}(h)/2\right]^{2\Lambda} dh \\ \breve{\sigma}_h^2(v) = \dfrac{1+2\Lambda}{\sqrt{\pi}} \displaystyle\int_{-\infty}^{+\infty} (h - \breve{m}_h)^2 e^{-h^2} \left[1 - \mathrm{erfc}(h)/2\right]^{2\Lambda} dh \end{cases} . \quad (21)$$

As Λ depends only on $v = \tan\phi/(\sqrt{2}\sigma_\gamma)$, $\breve{m}_h$ and $\breve{\sigma}_h$ depends also only on v. Since $\breve{m}_\xi = \sqrt{2}\sigma_\xi \breve{m}_h$ and $\breve{\sigma}_\xi = \sqrt{2}\sigma_\xi \breve{\sigma}_h$, $\{\breve{m}_\xi, \breve{\sigma}_\xi\}$ depends on $\{v(\phi, \sigma_\gamma), \sigma_\xi\}$. The advantage to use $\breve{m}_h$ and $\breve{\sigma}_h$ is to decrease the degrees of freedom for the simulations. They are plotted in Fig. 4 versus v. We observe that $\breve{m}_h$ is a decreasing function of v whereas $\breve{\sigma}_h$ is an increassing function of v. For very small grazing angles or very high slope standard deviations, which corresponds to small values of v, the illumination height PDF becomes narrow and it is shifted towards high heights. In constrast, when $v \geq 2$, $\breve{m}_h$ and $\breve{\sigma}_h$ become independent of v and tends to 0 and $1/\sqrt{2} = 0.707$, respectively. This means that $\breve{m}_\xi = \sqrt{2}\sigma_\xi \breve{m}_h = 0$ and $\breve{\sigma}_\xi = \sqrt{2}\sigma_\xi \breve{\sigma}_h = \sigma_\xi$ for any $\{\phi, \sigma_\gamma\}$. Thus, if $v \geq 2$, corresponding to a limit grazing incidence

angle $\phi_l = \arctan(2\sqrt{2}\sigma_\gamma)$, the shadowing effect can be neglected. For instance if $\sigma_\gamma = 0.1$, then $\phi_l = 15.8$ degrees. For the numerical results depicted in Section 5, $\sigma_\gamma = 0.15$ and $\sigma_\xi = 0.33$ meter. Thus, for $\phi = \{0.1, 2\}$ degrees, we have $v = \{0.008, 0.16\}$. From Fig. 4, $\breve{m}_h = \{1.7, 0.7\}$ and $\breve{\sigma}_h = \{0.3, 0.5\}$. Since $\sigma_\xi = 0.33$ meter, from (19), $\breve{m}_\xi = \{0.78, 0.32\}$ meter and $\breve{\sigma}_\xi = \{0.15, 0.24\}$ meter.

4. REFLECTION COEFFICIENT WITH SHADOW

As shown previously, for a rough surface illuminated by a plane wave at grazing angles, the shadowing effect increases the height mean value $\breve{m}_\xi(v(\phi, \sigma_\gamma), \sigma_\xi)$ of the illuminated surface (see Fig. 1). This height is function of the slope standard deviation, σ_γ, the grazing incident angle, ϕ, and the height standard deviation, σ_ξ.

The Ament reflection coefficient does not account for this phenomenon. It only modifies the strength field dynamics in the specular direction, and for the zone close to the ground it is equivalent to propagation over a flat surface. To include the influence of the shadowing effect, both approaches are developed here to suggest a new reflection coefficient through an "intuitive" and a "rigorous" approaches.

4.1. Intuitive Derivation of the Reflection Coefficient

The reflection coefficient defined by Ament [26] to take into account the surface roughness in the specular direction is

$$R_A(\phi) = R_0(\phi) \int_{-\infty}^{+\infty} e^{-jQ\xi} p_\xi(\xi) d\xi, \tag{22}$$

where $R_0(\phi)$ is the Fresnel reflection coefficient of a flat surface, and $Q = 2k_o \sin\phi$. Equation (22) can be seen as a phase correction in presence of roughness. If the shadow is ignored, the integration over ξ, corresponding to the derivation of the characteristic function, leading to

$$R_A(\phi) = R_0(\phi) \exp\left(-\frac{Q^2\sigma_\xi^2}{2}\right) = R_0(\phi) \exp\left(-2k_o^2\sigma_\xi^2 \sin^2\phi\right). \tag{23}$$

For $Q\sigma_\xi \ll 1$, the above equation is equal to the Fresnel reflection coefficient. In this case and ignoring the shadowing effect, the optical path correction can be neglected.

The increase of the surface mean level can be introduced in propagation modeling as a phase change of the plane wave to correct

the optical path. A simple solution is then to multiply the rough surface coefficient of Ament R_A [26] by a new phase term. This term expresses the difference in optical path between the cases of a rough and a smooth surface. The new reflection coefficient is then

$$R_I(\phi) = R_A(\phi)e^{-jQ\breve{m}_\xi}, \tag{24}$$

$\breve{m}_\xi = \sigma_\xi\sqrt{2}\breve{m}_h$ is the height mean level given by (21) and plotted in Fig. 4.

In Section 5, this approach will be compared with a Monte-Carlo method.

4.2. Rigorous Derivation of the Reflection Coefficient

To include the shadowing effect, another more rigorous technique consists in introducing the illumination height PDF $\breve{p}_S(\phi;\xi)$ given by (15) (valid for any uncorrelated process) and (16) (valid for an uncorrelated Gaussian process) into the derivation of the reflection coefficient. The derivation of this new reflection coefficient is identical to the method proposed by Ament [26, 6].

To obtain a reflection coefficient accounting for the shadowing effect, the height distribution $p_\xi(\xi)$ is substituted in (22) by the illumination height PDF, $\breve{p}_S(\phi;\xi)$, given for Gaussian statistics by (15) and (16). This leads to

$$\begin{aligned} R_R(\phi) = &\quad R_0(\phi)\int_{-\infty}^{+\infty} e^{-jQ\xi}p_S(\phi;\xi)d\xi \\ = &\quad R_0(\phi)\frac{1+2\Lambda}{\sqrt{\pi}}\int_{-\infty}^{+\infty} e^{-jQ\sqrt{2}\sigma_\xi h-h^2}\left[1-\frac{\mathrm{erfc}(h)}{2}\right]^{2\Lambda}dh \end{aligned} \tag{25}$$

This integral is computed numerically. To overcome this numerical computation, a last approach is proposed, fitting the rigorous illumination normalised height PDF and following (20) and (21), a new reflection coefficient is suggested:

$$R'_R(\phi) = R_0(\phi)\exp\left(-jQ\breve{m}_\xi - \frac{Q^2\breve{\sigma}_\xi^2}{2}\right). \tag{26}$$

Unlike (23), (25) and (26) have a non-zero phase term, due to the fact that the mean value of the illuminated height, $\breve{m}_\xi$, is non zero. If the shadowing effect is omitted, then $\breve{m}_\xi = 0$ and $\breve{\sigma}_\xi = \sigma_\xi$ and (26) is equal to (23). In addition, from Fig. 4, $\breve{\sigma}_\xi \leq \sigma_\xi \Rightarrow |R'_R(\phi)| \geq |R_A(\phi)|$.

Both approaches that we called intuitive (24) and rigorous (25) or (26), use the illumination height PDF allowing to include the mean enhancement of the height of the illuminated surface.

This new reflection coefficient R'_R is then introduced in (4) instead of the classical Fresnel coefficient R_0. This way, the DMFT will propagate the electromagnetic field taking into account the shadowing effect.

5. COMPARISONS ON PROPAGATION COMPUTATION

5.1. Test Description

The shadowing effect presented in the previous section is described for Gaussian statistics. With the aim to validate this approach, simulations of the propagation above deterministic surfaces with Gaussian statistics and Gaussian height correlation function are presented in this section. To generate this kind of surface, the standard deviations of the heights, σ_ξ, and of the slopes, σ_γ, are required. To obtain surfaces with characteristics close to a sea surface, the ElFouhaily et al. spectrum [29] is used to compute σ_ξ and σ_γ. For a fully-developed sea, Bourlier et al. [30] showed

$$\sigma_\xi \approx 6.28 \times 10^{-3} u_{10}^{2.02} \text{ in m} \quad \sigma_\gamma \approx 5.62 \times 10^{-2} u_{10}^{0.5}, \tag{27}$$

where u_{10} is the wind speed at 10 meters above the sea. A sea state of 4 on the Beaufort scale is chosen, giving a wind speed $u_{10} = 7\,\text{m/s}$. Thus, $\sigma_\xi = 0.33$ meter, $\sigma_\gamma = 0.15$ and the height correlation length is of the order of $L_c = \sqrt{2}\sigma_\xi/\sigma_\gamma \approx 3$ meters.

The propagation factor, for an horizontal polarization, is plotted along the vertical observation axis at a distance of 5 kilometers from the transmitter, which is located at 5 meters above the sea surface. Following these geometrical parameters, the observation height is growing from 0 to 200 meters, the grazing incidence angle ranges from near 0 to 2.3 degrees. The atmosphere is assumed to be homogeneous. The dielectric characteristics of the surface are 80.0 for the relative permittivity and 4.0 S/m for the conductivity. Four configurations are studied, and summarized in Table 1, in which N is the number of generated surfaces to obtain a good convergence of the mean propagated field. The radar frequency ranges from 1 to 10 GHz, involving a ratio $\frac{\sigma_\xi}{\lambda}$ ranged from 1.1 to 11. This criterion will allow to illustrate the influence of roughness on the propagation factor. These four configurations have been chosen to simulate realistic difficult propagation conditions at grazing angles where the shadowing effect is strong.

Table 1. Characteristics of the configurations.

Configurations	σ_γ	σ_ξ in m	Frequency (GHz)	σ_ξ/λ	N
1	0.15	0.33	1.0	1.1	100
2	0.15	0.33	2.5	2.75	200
3	0.15	0.33	5.0	5.5	300
4	0.15	0.33	10	11	500

5.2. Study of the Illumination Height PDF Choice

The analysis presented in Section 3 showed that the Smith formulation is the more accurate. The problem is to know if the correlation must be taken into account or not in the computation of the propagation factor. The formulation including the correlation in the illumination height PDF is given by (11) and (17), and can be compared to the uncorrelated one, (15) and (16). Both are introduced in the computation of the propagation factor within the reflection coefficient. The results presented here correspond to the configuration number 3 described in Table 1. Other cases have been tested and the conclusions are similar. In Fig. 5, the variation of the propagation factor with respect to the altitude is represented.

In the legend, the labels are defined as:

- "Rigorous Co Smith" means that in the computation of the reflection coefficient (25), the illumination height PDF is computed from the *correlated* Smith approach, (11) and (17).
- "Rigorous Un Smith" means that the reflection coefficient is computed from (25): the illumination height PDF is computed from the *uncorrelated* Smith approach.
- "Intuitive Un Smith" means that the reflection coefficient is computed from (24), in which the height mean value is determined from the uncorrelated Smith approach, (18) and (19).
- "Gaussian Un Smith" means that the reflection coefficient is given by (26).
- "Rigorous Un Smith PWS" will be explained later.

In Fig. 5, no significant differences can be distinguished between the results obtained with and without correlations. The only significative difference appears between the intuitive method and the others. The level difference observed when the propagation factor reaches the extrema is due to the second term in the exponential of (26) that is not taken into account in the intuitive method.

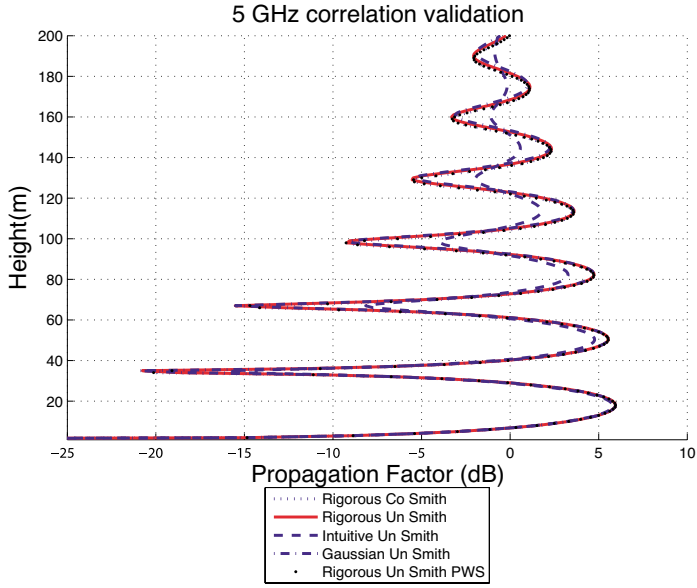

Figure 5. Test of the influence of the correlation between heights and slopes.

Indeed the propagation factor, P_F, can be approximated as, $P_F = 1+|R|^2+2|R|\cos(\phi_R+\Theta)$, in which R is the reflection coefficient, $\phi_R = \arg R$ and Θ is the phase difference between the direct path and the one reflected on the surface. It is then easy to show that the difference between the maxima ($\phi_R + \Theta = 2n\pi$ with n an integer) and the minima ($\phi_R + \Theta = 2n\pi + \pi/2$) of P_F is given by $\Delta_R = 4|R|$. From the intuitive approach, (24) plus (23), $\Delta_R = 4|R_0(\phi)|\exp(-Q^2\sigma_\xi^2/2)$ and from (26), $\Delta_R = 4|R_0(\phi)|\exp(-Q^2\breve{\sigma}_\xi^2/2)$. Since $\breve{\sigma}_\xi \leq \sigma_\xi$, Δ_R of the intuitive approach is smaller than the one of the rigorous approach.

The computation time induced by the processing of the correlated approach is much higher than the uncorrelated approach, because a triple integral computation is necessary. The conclusion of this test is that the Smith uncorrelated approach gives similar results as the correlated one and is preferred because of its computation time. The two method kept for the end of the study are the "intuitive" and the "Rigorous" approaches, in which the uncorrelated Smith formulation is used.

In the development of the reflection coefficient, the incident wave is approximated as a plane wave in the computation of the

modified impedance. This point seems to be a questionable hypothesis but a simple test can prove that it is correct. The spherical incident plane wave can be decomposed in its Plane Wave Spectrum (PWS) by applying a Fourier Transform. From this decomposition, each component of the spectrum is characterized by its direction of propagation. Considering this physical characteristic, and only computing the reflection within the specular component (so neglecting the diffraction on the rough surface) each component of the incident PWS can be reflected on the rough surface by considering image theory and by multiplying the incident PWS by the modified reflection coefficient. The complete reflected field can then be obtained by applying an inverse Fourier transform [28]. In Fig. 5, denoted in the legend as "Rigorous Un Smith PWS", this approach is compared with the others. The results are rigorously identical. This validates that the approximation of the incident wave to a plane wave in the impedance modeling is correct.

5.3. Monte Carlo Approach

For each realization of the surface, the propagation is computed using a DMFT algorithm by considering the terrain as irregular and deterministic, and then stored. An important remark is that the slope values of the generated surfaces do not exceed 15 degrees, because the slope standard deviation $\sigma_\gamma = 0.15$, corresponding to an angle of 8.5 degrees. Thus, the propagation above the generated surfaces is computed by applying the shift mapping approach, which is the more accurate. The propagation factor is then obtained by averaging those computed for each realization.

5.4. Comparison for different roughnesses

In this section, four methods are presented and compared :

- The first one uses the boundary condition computed from the Ament reflection coefficient without shadow expressed by (22).
- The second method is the reference based on a Monte Carlo process described in previous subsection.
- The third and fourth are denotes as "Intuitive Un Smith" and "Rigorous Un Smith", already exposed. It can be noticed that the "Rigorous Un Smith" approach could be substituted by the "Gaussian Un Smith" one, which gives similar results for a simplified formulation and a slightly smaller computation time.

Fig. 6 represents the average propagation factor with respect to the height above series of surfaces generated following the characteristics of

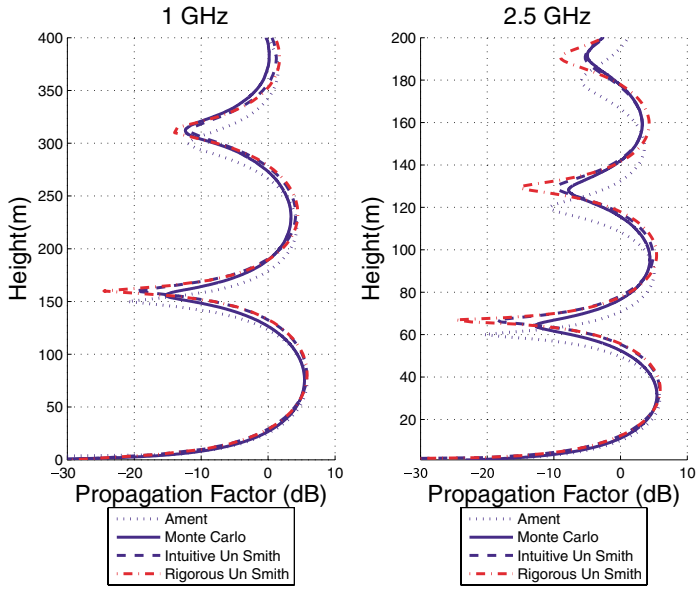

Figure 6. Propagation factor above Gaussian rough surface corresponding to a sea state 4. Configurations 1 and 2, Table 1.

the configurations 1 and 2 of Table 1. A rather good agreement can be observed between the Ament method without shadow and the others at 1GHz. This depicts the small influence of the shadowing effect when the ratio $\frac{\sigma_\xi}{\lambda}$ is close or lower than unity. At 2.5 GHz, a quite good agreement is obtained between the reference method (Monte Carlo) and the two methods based on the introduction of the illumination height PDF : the positions of maxima and minima of interference are better than with the Ament approach. In Fig. 6, we also observe that the dynamic of the propagation factor is different between Monte Carlo method and the others: the level is lower for the minima.

In Fig. 7, the same layout is plotted as previously corresponding to the configurations 3 and 4 of Table 1. A strong shift is observed between the minima and the maxima positions obtained by the Ament method and the others due to the influence of the shadowing effect.

The rigorous and intuitive methods give a good agreement with the reference solution. Whereas the positions of the interference lobes are very good, a problem on the level of the extreme values of the propagated field is observed at low altitudes. We have shown that the approximations made on the correlation of the illumination height PDF and on the incident wave (assumed to be a plane wave) had no

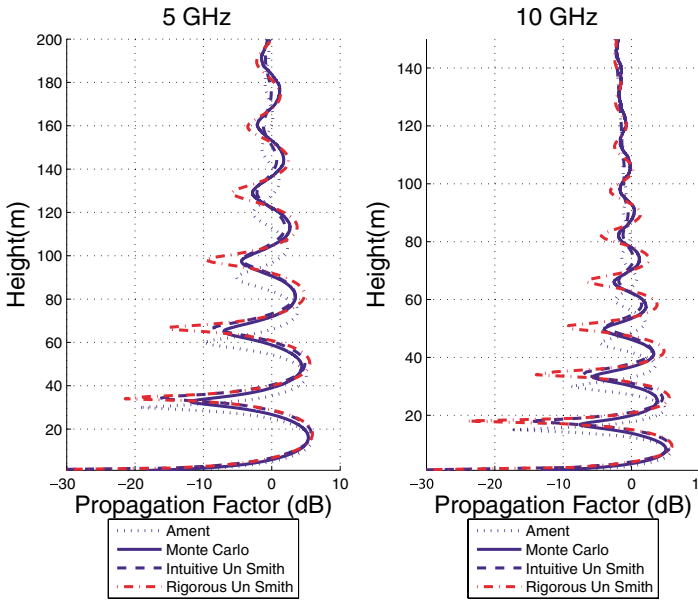

Figure 7. Propagation factor above Gaussian rough surface corresponding to a sea state 4. Configurations 3 and 4, Table 1.

effect on the results. So the difference of levels can be explained by the approximation of neglecting the diffraction that influences the dynamic of the field at low altitudes. Indeed, our approach considers only the specular direction of each facet of the surface.

In conclusion, the introduction of the shadowing effect into the reflection coefficient given by the Ament model allows to improve the results but it is not necessary when the standard deviation of the surface height σ_ξ is of the same order or lower than the wavelength. For ratio $\frac{\sigma_\xi}{\lambda}$ approximately ranging from 1 to 11, the results showed that the proposed method significantly improves the modeling of the propagation factor in term of the positions of the extreme values. The remaining problem with these approaches is that in the calculation of the boundary condition the diffraction is not taken into account. This phenomenon predicts a field level slightly higher for the maxima and lower for the minima.

Some other computations have been carried out above deterministic surfaces generated from a sea spectrum. A Monte Carlo process has been tested above these surfaces, and has given results very close to the ones presented in this paper.

5.5. Conclusion on Propagation Computation

In this section, the influence of the shadowing effect on the forward propagation above rough Gaussian surfaces has been presented. The modified reflection coefficient calculated in the previous section gives a better agreement with the statistical approach of Monte Carlo than the approach which neglects the shadowing effect. However, the following limitations of our approach appear: neglecting the diffraction influences the dynamic of the field. But for all the presented cases, the propagation modeling with shadowing effect give more accurate results than the Ament description and with very interesting computation time.

For example, on a standard PC Pentium 4 with 1 GHz of RAM the computation times obtained for the configuration 3 (see Table 1) is lower than 5 seconds and the same computation realised by the Monte Carlo process takes 70 minutes.

In operational conditions, the reflection coefficient used to model the forward propagation above the sea surface is the Miller and Brown model [26]. As the Ament reflection coefficient, the Miller and Brown [26] one doesn't take into account the shadowing effect, that creates a misplacement of extreme values of the propagation factor at grazing angles. So adding the shadow by using one of the proposed approaches can lead to a more powerful reflection coefficient. This interesting option is the way of further work.

6. CONCLUSION

A new reflection coefficient modelling rough surfaces forward scattering has been proposed. This one is derived from the Ament approach where the shadowing effect can be introduced statistically by different ways, giving intuitive and more rigorous models. It has been compared with the Ament coefficient and with a Monte Carlo approach as reference. This new reflection coefficient appeared to accurately represent electromagnetic propagation above rough surfaces. Indeed, the extreme value positions of the propagation factor are more accurately represented by our new approach.

Let us recall that the main point of interest of the proposed approach by comparison to more rigorous methods based on the method of moments [3–5], is the computing time and the memory space. The technique presented in this paper is useful for those who are trying to model long range radar propagation above rough ocean surfaces by taking into account the refraction atmosphere effects and the surface roughness.

APPENDIX A. EXPRESSIONS OF THE STATISTICAL ILLUMINATION FUNCTIONS FOR A CORRELATED GAUSSIAN PROCESS

For the expression of $g_{W,S}$ and $G_{W,S}$ it is convenient to use the following variable transformations

$$h = \frac{\xi}{\sqrt{2}\sigma_\xi} \quad \zeta = \frac{\gamma}{\sqrt{2}\sigma_\gamma} \quad u = \frac{x}{L_c} \quad v = \frac{\tan\phi}{\sqrt{2}\sigma_\gamma}, \tag{A1}$$

where σ_ξ and σ_γ are the standard deviations of the surface heights and slopes, and L_c is the surface height correlation length.

With the Wagner formulation, $g_W(\phi;\xi,\gamma,x)dx \equiv L_c g_W(v;h,\zeta,u)du$ is expressed as [19]

$$L_c g_W(v;h,\zeta,u) = \frac{\eta\sqrt{f_M}}{2\pi f_{33}} e^{-A-B}\left[1-\kappa\sqrt{\pi}e^{\kappa^2}\mathrm{erfc}(\kappa)\right]. \tag{A2}$$

The functions $\{A(v;h,\zeta,u), B(v;h,\zeta,u), \kappa(v;h,\zeta,u)\}$ are expressed as

$$\begin{cases} A = \left[f_{33}v^2 + 2v(f_{34}\zeta + f_{14}h - f_{13}h_1)\right] f_M^{-1} \\ B = \dfrac{f_{11}(h^2+h_1^2) + 2f_{12}hh_1 + 2\zeta(f_{13}h - f_{14}h_1) + f_{33}h^2}{f_M} \\ \qquad -h^2-\zeta^2 \\ \kappa = \dfrac{f_{14}h - f_{13}h_1 + f_{34}\zeta + f_{33}v}{\sqrt{f_{33}f_M}} \end{cases}. \tag{A3}$$

Moreover

$$h_1 = h + v\eta u. \tag{A4}$$

With the Smith formulation, $g_S(\phi;\xi,\gamma,x)dx \equiv L_c g_S(v;h,\zeta,u)du$ is expressed as

$$L_c g_S(v;h,\zeta,u) = \frac{\eta}{\pi}\frac{\sqrt{f_{11}f_{33}-f_{13}^2}}{f_{33}} \frac{e^{-A-B-h^2-\zeta^2}\left[1-\kappa\sqrt{\pi}e^{\kappa^2}\mathrm{erfc}(\kappa)\right]}{e^{B_1^2-C_1}\left[1+\mathrm{erf}\left(\sqrt{A_1}h_1+B_1\right)\right]}. \tag{A5}$$

The functions $A_1(u), B_1(h,\zeta,u), C_1(h,\zeta,u)$, which appear in the denominator, are expressed as [19]

$$\begin{cases} A_1 = (f_{11}f_{33} - f_{13}^2)/(f_{33}f_M) > 0 \\ B_1 = \dfrac{h(f_{12}f_{33} + f_{13}f_{14}) + \zeta(f_{13}f_{34} - f_{14}f_{33})}{\sqrt{f_{33}f_M(f_{11}f_{33} - f_{13}^2)}} \\ C_1 = h^2\dfrac{f_{11}f_{33} - f_{14}^2}{f_{33}f_M} + \zeta^2\dfrac{f_{33}^2 - f_{34}^2}{f_{33}f_M} + 2h\zeta\dfrac{f_{11}f_{33} - f_{14}f_{34}}{f_{33}f_M} \end{cases}. \tag{A6}$$

In the above equations, the functions $\{f_{ij}(u)\}$ which depend only on u, are expressed as

$$\begin{cases} f_{11} = 1 - f_2^2 - f_1^2 \\ f_{33} = 1 - f_0^2 - f_1^2 \\ f_{12} = f_0 f_2^2 + f_2 f_1^2 - f_0 \\ f_{34} = f_2 f_0^2 + f_0 f_1^2 - f_2 \\ f_{13} = f_1(f_0 - f_2) \\ f_{14} = f_1(1 - f_1^2 - f_0 f_2) \\ f_M = (f_{33}^2 - f_{34}^2)/(1 - f_0^2) \end{cases}, \tag{A7}$$

in which $\{f_0(u), f_1(u), f_2(u)\}$ are given by

$$f_0 = C_0/\sigma_\xi^2, \quad f_1 = -C_1/(\sigma_\xi \sigma_\gamma), \quad f_2 = -C_2/\sigma_\gamma^2. \tag{A8}$$

$C_0(x)$ denotes the surface height correlation function and $\{C_{1,2}(x)\}$ its first and second derivatives with respect to $x = uL_c$. In (A2) and (A5), $\eta = \sigma_\gamma L_c/\sigma_\xi$. For instance, for a Gaussian height correlation function, we have $C_0(x) = \sigma_\xi^2 \exp(-x^2/L_c^2)$, which implies that

$$\begin{cases} \sigma_s = \sqrt{-C_2(0)} = \sqrt{2}\sigma_\xi/L_c \\ \eta = \sqrt{2} \\ f_0 = \exp(-u^2) \\ f_1 = u\sqrt{2}\exp(-u^2) \\ f_2 = (1 - 2u^2)\exp(-u^2) \end{cases}. \tag{A9}$$

In Eq. (17), $x_t = u_t L_c$ corresponds to the lower value of u where the correlation can be neglected, which occurs for $f_0(u) \to 0$. For a Gaussian correlation function, $u_t = 3$. Above this limit, $\{f_0, f_1, f_2\} \approx \{0, 0, 0\}$, which implies from Eq. (A7) that $f_{ij} = 1$ for $i = j$, 0 otherwise and $f_M = 1$. The function g_W and g_S can then be simplified as

$$\begin{cases} L_c g_W = \dfrac{\eta v \Lambda e^{-(h+v\eta u)^2}}{\sqrt{\pi}} & = L_c g_W(v; h, u) \\ L_c g_S = \dfrac{2 g_W}{[1 + \mathrm{erf}(h + v\eta u)]} & = L_c g_S(v; h, u) \end{cases} \quad \text{for } u > u_t. \tag{A10}$$

In Eq. (17), $G_{W,S} = \exp\left[-\int_{u_t}^{+\infty} g_{W,S} du\right]$. Thus, the use of the above

equation leads to

$$\begin{cases} G_W(v;h,u_t) = \exp\left[-\dfrac{\Lambda}{2}\mathrm{erfc}(h+v\eta u_t)\right] \\ G_S(v;h,u_t) = \left[1-\dfrac{\mathrm{erfc}(h+v\eta u_t)}{2}\right]^{\Lambda} \end{cases} \quad \text{for } u > u_t. \qquad \text{(A11)}$$

If we assume that the above equation is valid for any u, which is similar to neglecting the correlation ($u_t = 0$), for $u_t = 0$, $G_W(v;h) = \exp\left[-\frac{\Lambda}{2}\mathrm{erfc}(h)\right]$ and $G_S(v;h) = [1-\mathrm{erfc}(h)/2]^{\Lambda}$. As $S_{W,S} = G_{W,S}^2$ in the forward direction, (12) (valid for any uncorrelated process) is found from (16), in which $F(\xi) = [1-\mathrm{erfc}(h)/2]$ with $h = \frac{\xi}{\sqrt{2}\sigma_\xi}$.

REFERENCES

1. Patterson, W. L., "A dvanced refractive effects prediction system (AREPS), version 1.0 users manual," Technical document 3028, Space and Naval Warfare Systems Center, 92152–5001, San Diego, CA, 1998.
2. Levy, M. F. and K. H. Craig, "TERPEM propagation package for operational forecasting with EEMS," *Proceedings of the 1996 Battelspace Atmospheric Conference,* 497–505, Technical Document 2938, NCCOSC, RDT and E Division, San Diego, 1996.
3. Rino, C. L. and H. D. Ngo, "Forward propagation in a half-space with an irregular boundary," *IEEE Trans. Ant. and Prop.*, Vol. 45, 1340–1347, 1997.
4. Ungan, B. U. and J. T. Johnson, "Time statistics of propagation over the ocean surface: A numerical study," *IEEE Trans. Geo. and Rem. Sens.*, Vol. 38, 1626–1634, 2000.
5. Lamar, M. T., R. S. Awadalla, and J. R. Kuttler, "An accelerated boundary integral equation scheme for propagation over the rough ocean surface," *Radio Science*, Vol. 37, No. 5, 2002.
6. Ament, W. S., "Toward a theory of reflection by a rough surface," *IRE Proc.*, Vol. 41, 142–146, 1953.
7. Freund, D. E., N. E. Woods, H.-C. Ku, and R. S. Awadallah, "The effects of the shadowing on multipath radar propagation modeling," *IEEE AP-S International Symposium and URSI National Radio Science Meeting*, Session No. 58, Washington, USA, July 3–5, 2005.
8. Dockery, G. D. and J. R. Kuttler, "An improved-boundary algorithm for Fourier split-step solutions of the parabolic wave

equation," *IEEE Trans. Ant. and Prop.*, Vol. 44, No. 12, 1592–1599, 1996.

9. Fock, V. A., "Solution of the problem of propagation of electromagnetic waves along the earth's surface by method of parabolic equations," *J. Phys. USSR*, Vol. 10, 13–35, 1946.
10. Hardin, R. H. and F. D. Tappert, "Application of the split-step Fourier method to the numerical solution of nonlinear and variable coefficient wave equations," *SIAM Rev.*, Vol. 15, 423, 1973.
11. Kuttler, J. R. and R. Janaswamy, "Improved Fourier transform methods for solving the parabolic wave equation," *Radio Science*, Vol. 37, No. 2, 2002.
12. Barrios, A. E., "Parabolic equation modeling in horizontally inhomogeneous environments," *IEEE Trans. Ant. and Prop.*, Vol. 40, 791–797, 1992.
13. Donohue, J. and J. R. Kuttler, "Propagation modeling over terrain using the parabolic wave equation," *IEEE Trans. Ant. and Prop.*, Vol. 48, 260–277, 2000.
14. Donohue, J. and G. D. Dockery, "Improved characterisation of low grazing angle sea clutter by the parabolic equation method," *RTO SET Symposium on Low Grazing Angle Clutter, Its Characterisation, Measurements and Application*, 30.1–30.13, 2000.
15. Leontovitch, A., "On the approximate boundary conditions for an electromagnetic filed on the surface of well-conducting bodies, investigations of propagation of radio waves," *Academy of Science*, Moscow, U.S.S.R, 1948.
16. Bass, F. G. and I. M. Fuks, "Calculation of shadowing for wave scattering from a statistically rough surface," *Sov. Radiophys.,* Vol. 7, 101–12, 1964.
17. Bass, F. G. and I. M. Fuks, *Wave Scattering from Statistically Rough Surfaces*, *International Series in Natural Philosophy,* C. B. Vesecky and J. F Vesecky (eds.), Pergamon, Oxford, 1979.
18. Kuznetsov, P. I., V. L. Stratonovich, and V. I. Tikhonov, "The duration of random function overshoots," *Sov. Phys. Tech. Phys.*, Vol. 24, 103, 1954.
19. Bourlier, C., G. Berginc, and J. Saillard, "Monostatic and bistatic statistical shadowing functions from one-dimensional stationary randomly rough surface according to the observation length: part I. Single scattering," *Waves Random Media*, Vol. 12, 145–174, 2002.
20. Wagner, R. J., "Shadowing of randomly rough surfaces,"

J. Acoust. Soc. Am., Vol. 41, 138–147, 1966.

21. Smith, B. G., "Lunar surface roughness, shadowing and thermal emission," *J. Geophys. Res.*, Vol. 72, 4059–4067, 1967.
22. Smith, B. G., "Geometrical shadowing of a random rough surface," *IEEE Trans. Ant. and Prop.*, Vol. 5, 668–671, 1967.
23. Beckman, P., "Shadowing of random rough surfaces," *IEEE Trans. Ant. and Prop.*, Vol. 13, 384–88, 1965.
24. Bourlier, C. and G. Berginc, "Shadowing function with single reflection from anisotropic Gaussian rough surface. application to Gaussian, Lorentzian and sea correlations," *Waves Random Media*, Vol. 13, 27–58, 2003.
25. Brokelman, R. A. and T. Hagfors, "Note of the effect of shadowing on the backscattering of waves from a random rough surface," *IEEE Trans. Ant. and Prop.*, Vol. 14, 621–627, 1967.
26. Brown, R. M. and E. V. Vegh., "New derivation for the rough-surface reflection coefficient and for the distribution of sea-wave elevations," *IEE Proc.*, Vol. 131, 114–115, 1984.
27. Hurtaud, Y., "Contribution à l'étude de la propagation des ondes millimétriques au-dessus de la mer," Ph.D. thesis, Université de Rennes, France, 1987.
28. Eibert, T. F., "Irregular terrain wave propagation by a fourier split-step wide-angle parabolic wave equation technique for linearly bridged knife-eidges," *Radio science*, Vol. 37, No. 1, 5.1–5.12, 2002.
29. Elfouhaily, T., B. Chapron, K. Katsaros, and D. Vandemark, "A unified directional spectrum for long and short wind-driven waves," *J. Geo. Res.*, Vol. 102, No. C7, 781–796, 1997.
30. Bourlier, C. and G. Berginc, "Microwave analytical backscattering models from randomly rough anisotropic sea surface — Comparison with experimental data in C and Ku bands," *Progress In Electromagnetic Research*, Vol. 37, 31–78, EMW Publishing, Cambridge, MA, 2002.